J Mater Sci (2009) 44:4613–4616
DOI 10.1007/s10853-009-3703-5

Synthesis and variable temperature electrical conductivity studies of highly ordered TiO_2 nanotubes

Ramazan Asmatulu · Annamalai Karthikeyan · David C. Bell · Shriram Ramanathan · Michael J. Aziz

Received: 21 March 2009 / Accepted: 22 June 2009 / Published online: 18 July 2009

Abstract Rafts of aligned, high aspect ratio TiO_2 nanotubes were fabricated by an electrochemical anodization method and their axial electrical conductivities were determined over the temperature range 225–400 °C. Length, outer diameter, and wall thickness of the nanotubes were approximately 60–80 μm, 160 nm, and 30 nm, respectively. Transmission electron microscopy studies confirmed that the TiO_2 nanotubes were initially amorphous, and became polycrystalline anatase after heat treatment at temperatures as low as 250 °C in air. The activation energy for conductivity over the temperature range 250–350 °C was found to be 0.87 eV. The conductivity values are comparable to those of nanocrystalline and nanoporous anatase thin films reported in literature.

Introduction

Titania is of tremendous interest for applications in photovoltaic devices such as solar cells [1, 2], photo-catalysis [3, 4], and photo-electrochemistry [5, 6]. For example, titania is a key component of the dye-sensitized solar cell (DSSC). TiO_2 is used to transport electrons from the light absorbing layer (such as $Ru(dcbpy)_2(NCS)_2$ dye) to the current collector. Recently, there has been tremendous interest in the use of nanocrystalline titania and mesoporous networks of titania in both DSSCs utilizing liquid electrolytes as well as solid-state solar cells [7–9]. Mesoporous titania networks are extensively used to investigate performance of solar cells, particularly the Grätzel cell [2] designs, and several approaches have been developed to fabricate nanostructured titania [7]. Nanotubes of titania have also attracted attention owing to their potential for application in photovoltaic devices [10].

In several of these technological applications, understanding the temperature dependent conductivity is critical for understanding device performance, as well as to extract fundamental information on conduction mechanisms and activation energy for carrier transport [11]. To the best of our knowledge, this study presents the first electrical conductivity measurements of titania nanotubes.

Experimental

The fabrication procedure followed closely the method of Grimes and coworkers [10, 12]. A 2 cm × 1.5 cm titanium foil (99.7%; Sigma-Aldrich) with a thickness of 250 μm was immersed into an etching solution containing 0.334 g of NH_4F (Sigma-Aldrich) dissolved into 2.2 mL of DI water and 97.47 mL of ethylene glycol (anhydrous, 99.8%; Sigma-Aldrich). The solution was mixed for about 15 min using a magnetic stirrer before the commencement of anodization. The Ti foil served as working electrode and a Pt counter electrode with the same lateral dimensions and a thickness of 200 μm was also immersed into the same solution facing the working electrode. A standard Ag/AgCl reference electrode was immersed in the solution and

R. Asmatulu · A. Karthikeyan · D. C. Bell · S. Ramanathan · M. J. Aziz (✉)
Harvard School of Engineering and Applied Sciences, Cambridge, MA 02138, USA
e-mail: maziz@harvard.edu

R. Asmatulu
Department of Mechanical Engineering, Wichita State University, 1845 Fairmount, Wichita, KS 67260-0133, USA

D. C. Bell
Center for Nanoscale Systems, Harvard University, Cambridge, MA 02138, USA

connected to the potentiostat. The distance between Ti foil and Pt foil was 3.8 cm and applied voltage ranged from 55 to 75 DC V between the working and reference was used for the anodization experiments.

After the anodization was complete, the TiO_2 nanotubes, which comprised yellow flakes on both sides of the Ti foil, were washed with isopropyl alcohol and then immersed in a diluted HCl (0.1 M) solution for 1 h to remove any unwanted deposits and surface impurities introduced during the anodization. Finally, the TiO_2 nanotubes were washed again with DI water and dried in an oven at 100 °C for a few hours.

Measurements of electrical conductivity through the film (i.e., along the axial direction of the nanotubes) were performed on pieces of flakes measuring about 1 mm × 1 mm. Devices were fabricated using silver electrodes on both sides and a stainless steel support plate. Electrodes were attached using pure silver enamel followed by a heat treatment at 70 °C. The stainless steel plate bearing the device was then mounted on a custom designed microprobe electrochemical system. Electrical conductivity measurements were performed in the frequency range of 300 kHz–0.1 Hz using a sinusoidal voltage signal. Conductivity was estimated as conductance divided by electrode area, ignoring the hollowness of the tubes.

Field emission scanning electron microscope (FESEM) images were obtained with a Zeiss 982 DSM. For Transmission electron microscopy (TEM), samples were prepared by dry crushing the bulk materials and depositing onto a "lacy carbon" coated TEM grid. The TEM used for obtaining the micrographs and diffraction patterns was a JEOL 2100 TEM operating at 200 kV.

Results and discussion

In Fig. 1 we present field emission scanning electron microscope (FESEM) images of TiO_2 nanotubes formed on the Ti metal surface. The TiO_2 nanotubes are approximately 60 μm long with 160 nm outer diameter and 30 nm wall thickness. It has been reported that increasing ammonium fluoride concentration, anodization potential and time result in longer nanotubes [11, 13]. However, we found that an anodization potential greater than 75 V caused dissolution of the surface of the Ti foil instead of the growth of titania nanotubes.

The mechanism of TiO_2 nanotubes formation in the NH_4F solution has been discussed by Mor et al. [10]. Oxide growth occurs due to the interaction of Ti with O^{2-} and hydroxyl ions and subsequent migration occurs due to an electric field gradient. Localized dissolution of the oxide due to the F^- ions similar to a corrosion process leads to pitting followed by pore growth (Fig. 1c). The tube formation occurs due to a geometric electric field intensity enhancement inside the pore region leading to vertical tube growth. Mor et al. have summarized the factors leading to tube array formation by considering the competition between electrochemical etching versus chemical dissolution in a recent review [10]. The tubes self-organize into a hexagonal array during growth. Indeed we observed a

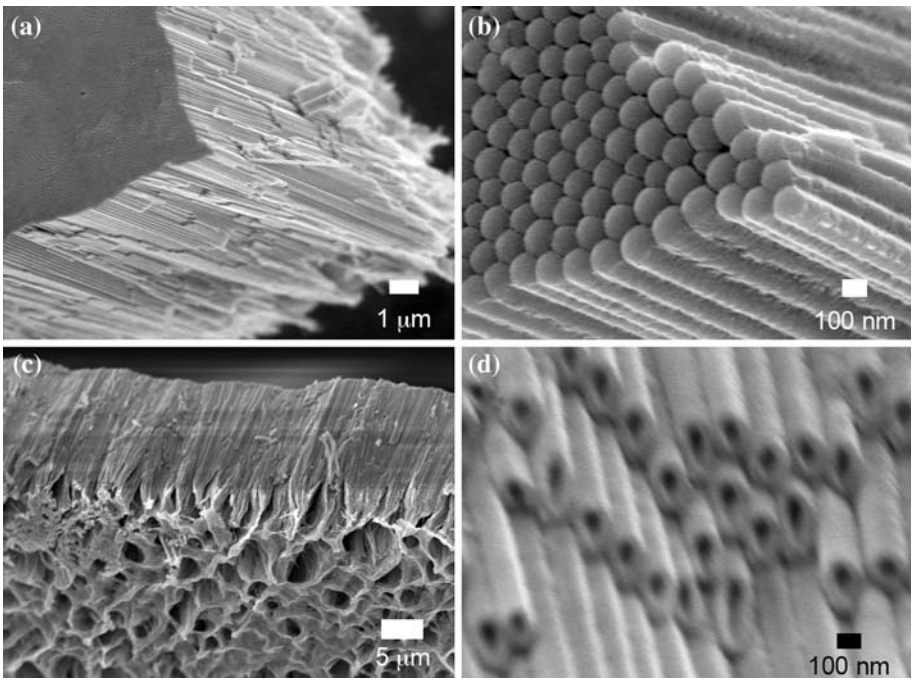

Fig. 1 FESEM images of flakes of TiO_2 nanotubes formed on the Ti foil after anodization at 55 VDC for 24 h. **a**, **b** "back" surface that was in contact with Ti foil before flake peel-off; **c**, **d** "front" or external surface. The distortion in (**d**) is due to charging of the sample during imaging

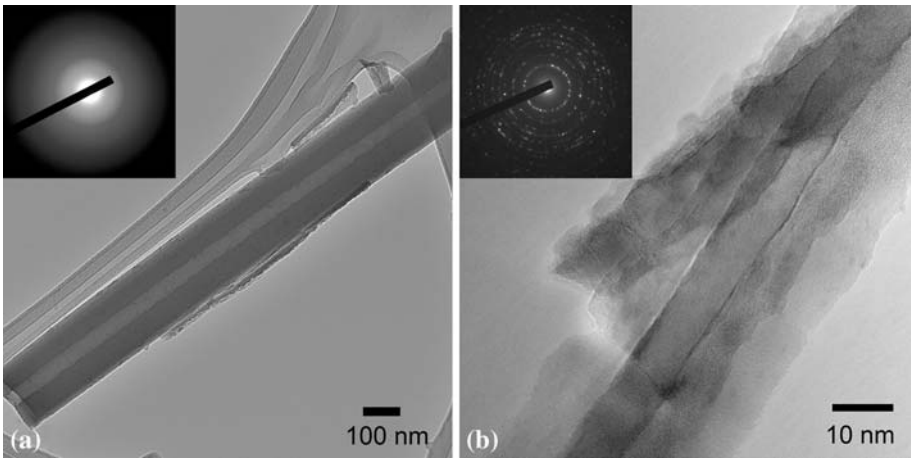

Fig. 2 TEM images of TiO_2 nanotube samples: **a** as-prepared, and **b** after 250 °C anneal in air. The insets are the corresponding selected area TEM diffraction patterns

hexagonal array of pits left on the surface of the Ti foil after the growth and removal of the flake of TiO_2 nanotubes.

TEM diffraction showed that the as-prepared TiO_2 nanotubes were originally amorphous, but after they had been heated to 225 °C in air, held at these conditions for temperature stabilization and electrical conductivity measurements (∼1 h), and cooled to ambient temperature, they were partly crystalline. Samples heated to 250 °C in air, held at these conditions for temperature stabilization and electrical conductivity measurements, and cooled to ambient temperature exhibited TEM diffraction patterns that appeared to be fully polycrystalline. Heating and cooling rates of the heat treatment were 1 °C/min. In Fig. 2 we present TEM images of an as-prepared nanotube (Fig. 2a) and of a 250 °C annealed nanotube (Fig. 2b). The corresponding TEM diffraction patterns from representative sample areas, obtained using a 500 nm selected area aperture, indicate amorphous and polycrystalline anatase, respectively. The first eight rings of the crystalline diffraction pattern, in order of increasing diameter, correspond to the 101, 004, 200, 105 + 211, 204, 220 + 116, 215, and 224 reflections of anatase. The grain size in Fig. 2b appears to be about 6 nm, but it is also possible that the apparent grain boundaries are actually tube fractures and more investigation needs to be done to clarify this interpretation.

The impedance plot recorded at different temperatures is shown as an inset in Fig. 3 in the form of an Nyquist plot. The high frequency part of the spectrum shows a semicircular arc as expected for an RC circuit. The lower frequency part is slightly extended. Polycrystalline titania samples usually show distinct or overlapping semicircular arcs corresponding to bulk and grain boundary responses. The as-prepared nanotubes are amorphous and are free from grain boundaries. However, the microstructures clearly show inter-tube boundary regions and such regions may contribute to distortions in low frequency part of the

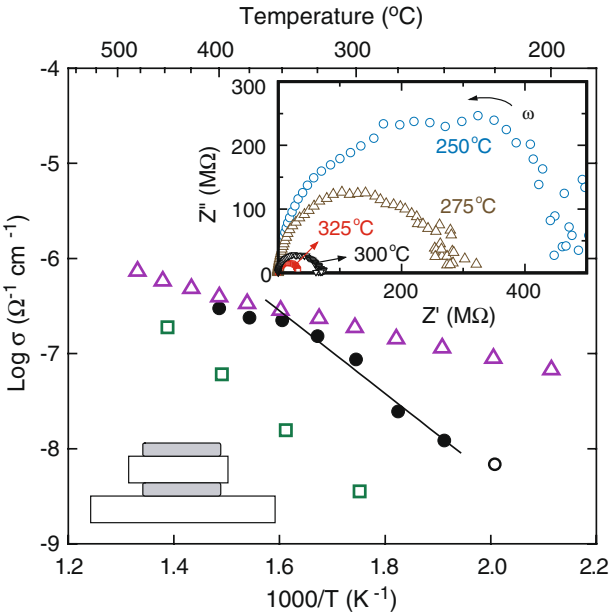

Fig. 3 Arrhenius plot of the electrical conductivity of TiO_2 nanotubes (*circles*) in air, with no prior annealing treatment. Sample measured at 225 °C has a significant amorphous component and is represented by an open circle. The line is fitted to the data from 250 °C through 350 °C. The insets show schematic of measurement geometry and impedance plots at several temperatures. Literature data for nanoporous anatase [14] (*squares*) and nanocrystalline anatase [15] (*triangles*) thin films are shown for comparison

impedance plot. The conductivity is obtained from the intercept of the impedance curve with the *x*-axis, taking into account the sample dimensions [13]. The electrical conductivity of the flakes is found to be $\sim 10^{-8}\ \Omega^{-1}\ \mathrm{cm}^{-1}$ at 300 °C. The electrical conductivity in the temperature range of 250–350 °C follows Arrhenius form with thermal activation energy of 0.87 eV. A deviation from the linear curve is observed above 350 °C. The electrical conductivity of the titania nanotubes is comparable to other forms of nanostructured titania. The activation energy observed below 350 °C is close to the values reported for

nanoporous anatase [14]. At higher temperatures, however, the activation energy and conductivity approach values reported for nanocrystalline anatase [15].

Summary

This work presents the fabrication and characterization of highly ordered TiO_2 nanotubes using the electrochemical anodization method. The conductivity of the TiO_2 nanotubes is between those of nanoporous and nanocrystalline anatase. The activation energy for electrical transport in TiO_2 nanotubes over the temperature range 250–350 °C was found to be 0.87 eV. These measurements pave the way for more comprehensive measurements of synthesis/structure/property relationships that are necessary for developing the understanding that is essential for optimal utilization of TiO_2 in energy applications.

Acknowledgements The authors gratefully acknowledge Craig Grimes and his group for helpful discussions and helping us to replicate their TiO_2 nanotube synthesis methods, Taeseok Kim for technical assistance and Changhyun Ko for indexing the diffraction pattern. The research of M. J. A. was supported in part by the U.S. Department of Energy grant DE-FG02-06ER46335. AK and SR acknowledge GCEP for financial support. This work was performed in part at the Center for Nanoscale Systems at Harvard University member of the National Nanotechnology Infrastructure Network (NNIN), which is supported by the National Science Foundation under NSF award no. ECS-0335765.

References

1. Wittmer H, Holten S, Kliem H et al (2000) Phys Stat Sol A Appl Res 181:2
2. Graetzel M, O'Regan B (1991) Nature 353:737
3. Diebold U (2003) Surf Sci Rep 48:53
4. Cardona AI, Candal R, Sanchez B et al (2004) Energy 29:845
5. Shaw K, Christensen P, Hamnett A (1996) Electrochim Acta 41:719
6. Kozuka H, Takahashi Y, Zhao GL et al (2000) Thin Solid Films 358:172
7. Zukalova M, Kavan L, Zukal A, Nazeeruddin MK, Liska P, Gratzel M (2005) Nano Lett 5:1789
8. Cahen D, Bisquert J, Hodes G, Ruhle S, Zaban A (2004) J Phys Chem B 108:8106
9. Kijitori Y, Miyasaka T (2004) J Electrochem Soc 151:A1767
10. Mor GK, Varghese OK, Paulose M et al (2006) Sol Energy Mater Sol Cells 90:2011
11. Frank AJ, Kopidakis N, van de Lagemat J (2004) Coord Chem Rev 248:1165
12. Shankar K, Mor GK, Prakasam H, Yoriya ES, Paulose M, Varghese OK, Grimes CA (2007) Nanotechnology 18:065707
13. Gerhardt R (1994) J Phys Chem Solids 55:1491
14. Dittrich T, Weidmann J, Koch F et al (1999) Appl Phys Lett 75:3980
15. Huber B, Brodyanski A, Scheib M et al (2005) Thin Solid Films 472:114